Available online at www.sciencedirect.com
SCIENCE DIRECT®
PERGAMON
Polyhedron 22 (2003) 375–381
POLYHEDRON
www.elsevier.com/locate/poly

Synthesis and spectroscopic identification of new iron(III) complexes with 5-methyl-3-formylpyrazole-3-piperidinylthiosemicarbazone (HMP_z3Pi): X-ray structure of $[Fe(MP_z3Pi)_2]ClO_4\cdot 2H_2O$

Nitis Chandra Saha [a], Ray J. Butcher [b], Siddhartha Chaudhuri [c], Nityananda Saha [a,1,*]

[a] *Department of Chemistry, University of Calcutta, 92 Acharya Prafulla Chandra Road, Kolkata 700009, India*
[b] *Department of Chemistry, Howard University, Washington, DC, USA*
[c] *R.S.I.C., Bose Institute, Kolkata 700009, India*

Received 19 April 2002; accepted 9 October 2002

Abstract

New iron(III) complexes of 5-methyl-3-formylpyrazole-3-piperidinylthiosemicarbazone (HMP_z3Pi), $[Fe(MP_z3Pi)_2]X\cdot 2H_2O$ (X = Cl, ClO_4 and NO_3) have been synthesised and physico-chemically characterised by magnetic data (polycrystalline state), electronic, IR and EPR spectral studies. Each of the reported species is a cationic complex (1:1 electrolyte) containing two moles of monodeprotonated title ligand and an anionic counterpart. IR spectra (4000–200 cm^{-1}) indicate coordination to the central iron(III) ion via the pyrazolyl (tertiary) ring nitrogen, azomethine nitrogen and thiolato sulfur atoms of the primary ligand molecule. EPR data (RT and LNT) show the presence of a low spin iron(III) cation with $d^2_{xz}\ d^2_{yz}\ d^1_{xy}$ configuration. X-ray crystallographic data of $[Fe(MP_z3Pi)_2]ClO_4\cdot 2H_2O$ ($P\bar{1}$, triclinic) have authenticated a FeN_4S_2 octahedral coordination as envisaged from spectral data. In the complex species, the two azomethine nitrogen atoms are *trans* to each other, while the pyrazolyl ring nitrogens and the thiolato sulfurs are in *cis* positions.

Keywords: Iron(III) complexes; Synthesis; Pyrazolylthiosemicarbazone; X-ray crystal structures

1. Introduction

The well-documented biological activities of several heterocyclic thiosemicarbazones have often been attributed to a chelation phenomenon with trace metal ions [1–4]. The success in therapeutic applications of *N*-heterocyclic thiosemicarbazones [3,5,6] for removing excess iron from iron-loaded mice through chelation therapy is quite remarkable. Further researches have been initiated in this specific area for such findings. In continuation of our earlier reports on iron(III) complexes [7] and related publications on first-row transition metal ion complexes of pyrazolyl thiosemicarbazones and dithiocarbazates [8], this communication reports the synthesis and spectroscopy of iron (III) complexes with the title ligand (HMP_z3Pi) together with the X-ray crystal structure of $[Fe(MP_z3Pi)_2]ClO_4\cdot 2H_2O$.

2. Experimental

All reagents and solvents were of AR grade and were obtained from commercial sources and used without further purification. Spectrograde solvents were used for physico-chemical measurements.

2.1. Preparation of 5-methyl-3-formylpyrazole-3-piperidinylthiosemicarbazone (HMP_z3Pi)

The title ligand (Fig. 1) was synthesised for the first time by a method similar to that reported earlier [9], but appropriately modified, followed by a final transamination [10] of the *S*-methyldithiocarbazate of 5-methyl-3-formylpyrazole (HMP_zSMe) with piperidine. The yel-

* Corresponding author. Present address: University of Kalyani, Kalyani 741235, India. Fax: +91-33-5828-282.
E-mail address: n.saha@cucc.ernet.in (N. Saha).
[1] nsaha2@yahoo.com.

0277-5387/02/$ - see front matter © 2002 Elsevier Science Ltd. All rights reserved.
PII: S0277-5387(02)01342-6

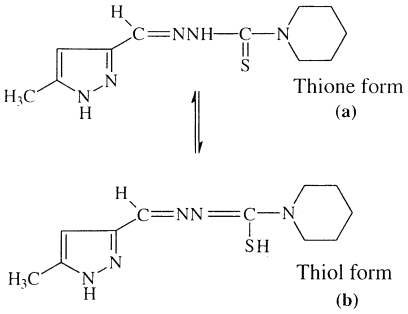

Fig. 1. Structural formulation of HMP_z3Pi.

lowish white crystalline product (from ethanol) melted at 159–161 °C. Yield ~55%. Found: C, 52.6; H, 6.7; N, 27.6 and calculated for $C_{11}H_{17}N_5S$: C, 52.5; H, 6.7; N, 27.8%. ^{1}H NMR δ(DMSO-d_6) 2.18 (3H, s), 6.21 (1H, s), 8.01 (1H, s), 10.84 (1H, b), 3.77 (4H, bs), 1.56 (6H, bs); *m/z* 251 (M^+, 60%).

2.2. General method of preparation of iron(III) complexes: $[Fe(MP_z3Pi)_2]X\cdot 2H_2O$ ($X = Cl$, ClO_4 and NO_3)

An ethanolic solution of the appropriate iron(III) salt (0.000525 mole) [anhydrous $FeCl_3$/$Fe(ClO_4)_3\cdot 6H_2O$/$Fe(NO_3)_3\cdot xH_2O$ (prepared in situ from freshly precipitated $Fe_2O_3\cdot xH_2O$ and dilute HNO_3)] was added to a hot solution of the title ligand (0.00105 mole) in the same solvent. The resulting dark brown solution was heated under reflux for approximately 30 min. On slow evaporation at room temperature (~30 °C), the precipitated dark brown iron(III) complex, in each case, was filtered off, washed thoroughly with cold ethanol and dried over anhydrous calcium chloride. Yield: 65–75%; satisfactory C, H, N analyses and data for iron-content of the complexes were compatible with the desired elemental compositions of the species (Table 1).

Note:

i) Caution! Perchlorate compounds are potentially explosive and should be handled with care.
ii) Dark brown needle-shaped crystals for the perchlorate complex, suitable for X-ray diffraction, were grown from ethanol.

2.3. Physical measurements

Elemental analyses (C, H and N) were done with a Perkin–Elmer 2400 CHNS/O analyser and the iron-content of the complexes was determined titrimetrically. The molar conductances of the complexes in methanolic solutions were measured with a Systronics 304 digital conductivity meter. Magnetic susceptibilities were measured in the polycrystalline state on a PAR 155 sample vibrating magnetometer. The ^{1}H NMR spectrum for the ligand was recorded in DMSO-d_6 with a Bruker AM 300L (300 MHz) superconducting FT NMR. The mass spectrum of the ligand was recorded with a JEOL JMS-D300 mass spectrometer. The electronic spectra (both DRS and solution) were recorded on a Hitachi U-3501 spectrophotometer. IR spectra (4000–200 cm^{-1}) were recorded on a JASCO FT/IR-420 spectrophotometer with KBr pellets. The EPR spectra were recorded on a Varian model E-112 spectrophotometer (X-band) in the polycrystalline state at RT and in MeOH at LNT using DPPH ($g = 2.0037$) as a standard.

2.4. Structure determination

X-ray diffraction data of the complexes were collected on a Bruker P4 diffractometer using Mo Kα radiation. The data were corrected for Lorentz, polarisation and absorption effects.

The structure was solved by direct methods using SHELXS [11] and refined by the full-matrix least-squares method based on $|F_{obs}|^2$ using SHELXL [11]. The non-hydrogen atoms were refined anisotropically, while the hydrogen atoms, either located from difference electron density maps or generated using idealised geometry, were made to 'ride' on their parent atoms and used in the structure factor calculations. Neutral atom scattering factors were taken from Cromer and Weber [12] and anomalous dispersion effects were included in F_{calc} [13]. The crystallographic data are summarised in Table 4. The final positional and thermal parameters are available as supplementary material.

Table 1
Elemental analyses, colours and other pertinent physico-chemical properties of the Fe(III) complexes

Complex (colour)	Elemental analyses Found (Calc.)				Conductivity at 30 °C in MeOH (Ω^{-1} cm^2 mol^{-1})	μ_{eff} (BM) at 298 K
	% C	% H	% N	% Fe		
$[Fe(MP_z3Pi)_2]Cl\cdot 2H_2O$ (dark brown)	42.3 (42.1)	5.7 (5.7)	22.5 (22.3)	8.8 (8.9)	115	2.2
$[Fe(MP_z3Pi)_2]ClO_4\cdot 2H_2O$ (dark brown)	38.1 (38.2)	5.2 (5.2)	20.3 (20.2)	8.2 (8.1)	110	1.9
$[Fe(MP_z3Pi)_2]NO_3\cdot 2H_2O$ (dark brown)	40.6 (40.3)	5.5 (5.5)	23.2 (23.5)	8.3 (8.5)	112	2.0

3. Results and discussion

3.1. Characterisation of 5-methyl-3-formylpyrazole-3-piperidinylthiosemicarbazone (HMP$_z$3Pi)

The title ligand, HMP$_z$3Pi, has been characterised by elemental analyses (C, H and N), IR, ^{1}H NMR and mass spectrum. The ligand shows the characteristic IR bands (cm^{-1}) at 3300–3250 (ν_{NH}), 1610 (ν_{CH-N}), 1525 (ν_{C-N}), 1040 (ν_{N-NPZ}) and 860 (ν_{C-S}) which are in good agreement with the structural formulation as in Fig. 1(a). The ligand molecule contains a proton adjacent to the thiocarbonyl group and consequently can exhibit thione-thiol tautomerism. The IR spectrum of the free ligand does not show any (ν_{SH}) band in the region 2600–2200 cm^{-1}. This indicates that the thiol tautomer is absent in the solid state [14,15]. The spectrum shows bands in the region 3300–3250 cm^{-1}, indicating the existence of only the thio-ketotautomer (Fig. 1(a)). The ^{1}H NMR spectrum of the free ligand in DMSO-d_6 gives singlets at δ 2.18 (3H) and δ 6.21 (1H) assigned to C_5–CH_3 and C_4–H of the pyrazole ring, respectively. The one-proton singlet at δ 8.01 is ascribed to –CH–N–. The spectrum exhibits a low field signal, at $\delta = 12.72$, which is due to the formation of the S–H bond indicating the thione-thiol tautomerism of the ligand in solution [16]. Another singlet at $\delta = 10.84$ is due to the hydrazinic proton (–NH–). From the integral intensity of hydrazinic and thiol proton signals, it is observed that the thione–thiol (Fig. 1) remain in equilibrium and the ratio is approximately 2:1 in favour of the former. Two broad singlets at $\delta = 3.77$ and $\delta = 1.56$ are assigned to the ortho hydrogens and meta/para hydrogens of the piperidine ring, respectively.

The mass fragmentation data are compatible with the proposed molecular formula, $C_{11}H_{17}N_5S$. The strongest molecular ion peak appears at m/z 251 (M^+ 60%).

3.2. Characterisation of the iron(III) complexes

All these iron(III) complexes give satisfactory C, H, N and Fe analyses and conform to the general composition, [Fe(MP$_z$3Pi)$_2$]X·2H$_2$O (X = Cl, ClO_4 and NO_3). The molar conductance values in MeOH (30 °C) indicate 1:1 electrolytic character of the complexes [17]. The complexes are paramagnetic ($\mu_{eff} = 1.9 \sim 2.2$ BM at 25 °C) for a low spin d^5 ion (Table 1).

3.2.1. Vibrational and electronic spectra

The characteristic IR bands (4000–200 cm^{-1}) for the free ligand, when compared with those of its iron(III) complexes, provide positive indications with regard to the bonding sites of the primary ligand molecule (Table 2) and the information are in conformity with our previous findings [7]. A negative shift in $\nu_{(CH-N)}$ band ($\sim$1610 cm^{-1}) in the spectrum of the free ligand to lower values (1590–1575 cm^{-1}) in its complexes is consistent with coordination of the azomethine nitrogen to the central Fe(III) ion. The IR bands at 470–485 cm^{-1} in the complexes are then assignable to $\nu_{(Fe-N)}$ [17]. IR bands at around 1630–1620 cm^{-1}, assignable to $\nu_{(C-N)}$ in the complexes, are due to the generation of a double bond between ^{2}N and ^{3}C (i.e. –N–^{2}NH–^{3}C(S)–^{4}N<) as the proton attached to the ^{2}N atom of the thiosemicarbazone moiety is lost during complexation. An intense band at 860 cm^{-1} in the free ligand spectrum, assigned to $\nu_{(C-S)}$, has been found to shift to lower frequency regions (785–770 cm^{-1}) in the complexes, indicating the coordination of the thiol sulfur to Fe(III); moreover, the appearance of a new band in the region (380–365 cm^{-1}) in the complexes is assignable to $\nu_{(Fe-S)}$ [8d]. The free ligand bands at 1525 and 630 cm^{-1}, assignable to $\nu_{(C-N)}$ (pyrazole ring) and the in-plane deformation of the pyrazole ring, respectively, have been found to shift to the higher frequency region, suggesting that the tertiary ring nitrogen atom (^{2}N) is a bonding site [7,18,19]. The bands around 295–280 cm^{-1} in the complexes are then clearly assignable to $\nu_{(Fe-N)}$ (pyrazole ring) [8d].

The diffuse reflectance spectral data of the iron(III) complexes show three main bands in the regions 20 400–19 950, 17 400–16 270 and 11 200–10 910 cm^{-1}; these bands can be tentatively assigned to a $^2T_2$ ground state for the iron(III) ion. The intense bands at 20 400–19 950 cm^{-1} and 17 400–16 270 cm^{-1} may be attributed to CT transitions arising from the d$\rightarrow\pi^*$ transition. The d–d transition bands at 11 200–10 910 cm^{-1} might correspond to a $^2T_2 \rightarrow {}^2T_1$ transition [20,21]. The electronic spectra of the complexes in methanol exhibit three bands in the region 20 100–19 270, 16 500–15 920 and 11 050–10 595 cm^{-1}. Bands visible between 20 100 and 15 920

Table 2
Selected IR bands (cm^{-1}) for the ligand and its Fe(III) complexes pertaining to coordination sites

Compound	$\nu_{(CH-N)}$ (azomethine)	$\nu_{(C-N)}$ (pyrazole)	$\nu_{(C-S)}$	$\nu_{(Fe-N)}$ (azomethine)	$\nu_{(Fe-N)}$ (pyrazole)	$\nu_{(Fe-S)}$
HMP$_z$3Pi	1610	1525	860			
[Fe(MP$_z$3Pi)$_2$]Cl·2H$_2$O	1575	1545	780	470	287	369
[Fe(MP$_z$3Pi)$_2$]ClO$_4$·2H$_2$O	1590	1540	770	485	295	365
[Fe(MP$_z$3Pi)$_2$]NO$_3$·2H$_2$O	1584	1542	779	478	280	380

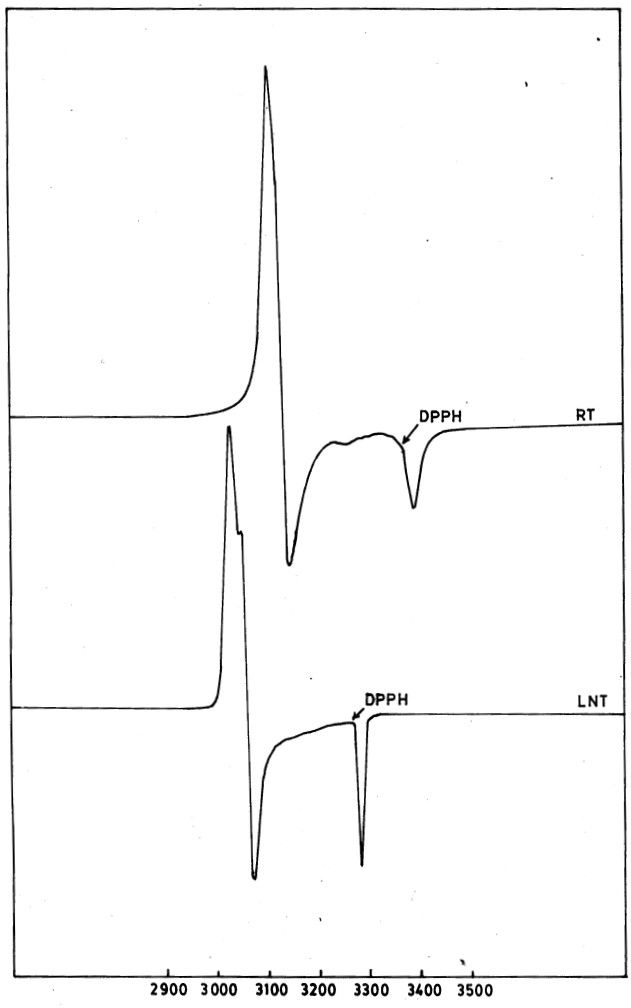

Fig. 2. X-band EPR spectra of $[Fe(MP_z3Pi)_2]NO_3\cdot 2H_2O$ at RT and LNT.

cm^{-1} are likely due to $d\rightarrow\pi^*$ metal to ligand as well as sulfur to Fe(III) transitions [6,22]. The bands at 11 050–10 595 cm^{-1} can be designated as d–d transition bands of a spin-paired d^5 species with a distorted octahedral structure [23,24].

3.2.2. EPR spectra

The EPR spectral parameters for the complexes at RT (298 K) and under frozen conditions (77 K), in solid and in solution (MeOH), confirm the low spin character of the iron(III) ions. In the solid (polycrystalline) state, all the complexes exhibit axial spectra, but in frozen condition, they show well-defined rhombic spectra with three g values; representative spectra for $[Fe(MP_z3Pi)_2]NO_3\cdot 2H_2O$ at RT and LNT are shown in Fig. 2. The g values of the complexes along with those of g_{av} are shown in Table 3. It is observed that the g values of the complexes in frozen condition are slightly higher than those at RT, but the deviation is not so significant as to account for the changed electronic configuration and alteration of Fe(III) centres in solution [23]; this slight deviation may be due to lattice effects. In conjugation with the solid state effects due to involvement of the anions, the symmetry of the spectra is lifted and gives a rhombic symmetry. This rhombic distortion is common in spin-paired iron(III) complexes [23,24]. The highest g values do not suffer super-hyperfine splitting; this indicates the absence of any interaction between the unpaired electron and the imine nitrogen [25]. The deviation of g values from 2.0037 indicates that the unpaired electron is in the d_{xy} orbital [26] with $d^2_{xz}d^2_{yz}d^1_{xy}$ configuration of the low spin iron(III) cations.

3.3. Crystal structure of $[Fe(MP_z3Pi)_2]ClO_4\cdot 2H_2O$

The ORTEP [27] diagram of the complex (Fig. 3) shows the atom numbering scheme. The iron(III) ion has a distorted octahedral coordination in the complex. Two molecules (designated as A and B) of the monodeprotonated tridentate ligand, 5-methyl-3-formylpyrazole-3-piperidinylthiosemicarbazone (MP_z3Pi^-), coordinate to the Fe(III) ion via the pyrazolyl (tertiary) nitrogens [N(1A) N(1B)], the azomethine nitrogens [N(2A), N(2B)], and the thiolato sulfurs [S(1A), S(1B)], to form four five-membered chelate rings [Fe–S(1A)–C(6A)–N(3A)–N(2A), Fe–S(1B)–C(6B)–N(3B)–N(2B), Fe–N(1A)-C(4A)–C(5A)–N(2A) and Fe–N(1B)–C(4B)–C(5B)–N(2B)]. The pattern of coordination is similar to that observed in the crystal structure of the Fe(III) complex of 2-pyridineformamide 3-piperidylthiosemicarbazone $[Fe(Ampip)_2]ClO_4$ [28]. The crystallographic asymmetric unit consists of a $[Fe(MP_z3Pi)_2]^+$ cation, a perchlorate anion and two molecules of water of

Table 3
EPR spectral parameters for the complexes

Complex	State	Temperature	g values			g_{av}
$[Fe(MP_z3Pi)_2]Cl\cdot 2H_2O$	solid	RT	$g_{\parallel}=2.146$		$g_{\perp}=1.935$	2.076
	MeOH	LNT	$g_1=2.177$	$g_2=2.157$	$g_3=1.987$	2.107
$[Fe(MP_z3Pi)_2]ClO_4\cdot 2H_2O$	solid	RT	$g_{\parallel}=2.153$		$g_{\perp}=1.944$	2.049
	MeOH	LNT	$g_1=2.160$	$g_2=2.142$	$g_3=1.997$	2.099
$[Fe(MP_z3Pi)_2]NO_3\cdot 2H_2O$	solid	RT	$g_{\parallel}=2.159$		$g_{\perp}=1.990$	2.103
	MeOH	LNT	$g_1=2.162$	$g_2=2.139$	$g_3=1.994$	2.098

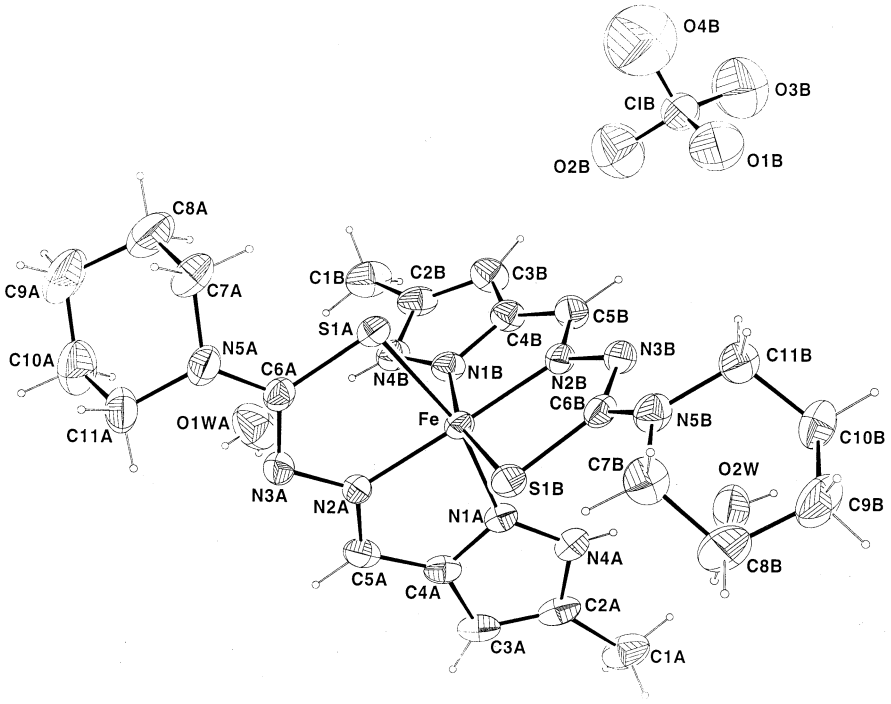

Fig. 3. ORTEP plot of $[Fe(MP_z3Pi)_2]ClO_4 \cdot 2H_2O$ showing the atom numbering scheme. Thermal ellipsoids are shown at 30% probability.

crystallisation. The perchlorate anion and one of the water molecules are disordered.

Selected bond distances and angles are shown in Table 5. There is a slight shortening of the Fe–N(azomethine) distances compared with the Fe–N(pyrazolyl) distances (Table 5); this may be attributed to the fact the azomethine nitrogen is a stronger base compared with the pyrazolyl nitrogen. A similar effect has also been observed in the structure of $[Fe(Ampip)_2]ClO_4$ [Fe–N(azomethine) 1.911(3), 1.913(3) Å; Fe–N(pyridine) 1.998(3), 2.008(3) Å] [28].

The two azomethine nitrogen atoms [N(2A) and N(2B)] are *trans* to each other, while the pyrazolyl ring nitrogen atoms [N(1A) and N(1B)] and the thiolato sulfur atoms [S(1A) and S(1B)] are in *cis* positions. This configuration about the central Fe(III) ion is found to be identical to that in $[Fe(Ampip)_2]ClO_4$ [28].

The two coordinating ligands are more or less planar, with C(3A) and N(3A) in ligand A, and C(6B) and C(4B) in ligand B, having the largest deviations in opposite directions [C(3A): +0.175(2) Å, N(3A): −0.150(2) Å, C(6B): +0.131(5) Å, and C(4B): −0.100(5) Å] from the least-squares mean planes through Fe–S(1)–C(6)–N(3)–N(2)–C(5)–C(4)–C(3)–C(2)–N(4)–N(1). The ligands A and B coordinate orthogonally to the metal ion, the dihedral angle between them being 91.40(3)°. The three individual rings in either ligand, namely the pyrazole and the two five-membered chelate rings, are individually almost planar with small dihedral angles between them. The maximum dihedral angle of 8.02(8)° is between the pyrazole ring N(1A)–N(4A)–C(2A)–C(3A)–C(4A) and the chelate ring Fe–S(1A)–C(6A)–N(3A)–N(2A).

While comparing the structure of $[Fe(MP_z3Pi)_2]ClO_4 \cdot 2H_2O$ with that of $[Fe(Ampip)_2]ClO_4$ [28], it is observed that there are striking similarities between the two, except that there are certain differences in the Fe–N bond distances involving the azomethine and the ring nitrogens (pyrazolyl or pyridyl). The Fe–N(azomethine) bond distances are slightly shorter in $[Fe(Ampip)_2]ClO_4$; this is probably due to the presence of the NH_2 groups on the carbon atoms adjacent to the azomethine nitrogens, making them harder bases. On the other hand, the Fe–N(pyrazolyl) distances are shorter in the present case compared with the Fe–N(pyridyl) distances in $[Fe(Ampip)_2]ClO_4$. This is perhaps due to the fact that the pyrazolyl (tertiary) nitrogen is a stronger nucleophile.

The piperidine rings of both the coordinating ligands are in the chair conformation [29]: in ligand A, $q_2 = 0.038(9)$ Å, $q_3 = 0.554(9)$ Å, $Q = 0.556(9)$ Å, $\theta = 4.4(9)°$, and in ligand B, $q_2 = 0.058(8)$ Å, $q_3 = 0.558(8)$ Å, $Q = 0.561(8)$ Å, $\theta = 5.2(8)°$.

Table 6 gives the details of the hydrogen bonding contacts. The two pyrazolyl nitrogen atoms are the donors in N–H···O hydrogen bonds to two water molecules. One of the water molecules, O(2W), donates its protons to a perchlorate oxygen, O(1B), and a hydrazinic nitrogen, N(3B), to form O–H···O and O–H···N hydrogen bonds. The protons from the major

Table 4
Crystal data

Empirical formula	$C_{22}H_{36}ClFeN_{10}O_6S_2$
Formula weight	692.05
Crystal colour	Dark brown
Temperature (K)	296(2)
Wavelength (Å)	0.71073
Crystal system	Triclinic
Space group	$P\bar{1}$
Unit cell dimensions	
a (Å)	9.284(1)
b (Å)	12.360(2)
c (Å)	14.995(2)
α (°)	74.621(9)
β (°)	72.315(9)
γ (°)	86.713(10)
Volume (Å^3)	1580.2(3)
Z	2
$F(000)$	722
Crystal size (mm)	$0.22 \times 0.32 \times 0.51$
θ Range for data collection (°)	2.3–27.5
Index ranges	$0 \le h \le 12$, $-15 \le k \le 15$, $-18 \le l \le 19$
Reflections collected	7480
Independent reflections	7062 [$R_{int} = 0.033$]
μ (mm^{-1})	0.747
Absorption correction	SHELXA
Max/min transmission	0.0404, 0.0289
Refinement method	full-matrix least-squares on F^2
Observed reflectons	4550
Number of parameters	485
Number of restraints	77
Goodness-of-fit on F^2	1.04
Final R indices ('observed' data) [a]	$R_1 = 0.0716$, $wR_2 = 0.1960$
Final R indices (all data)	$R_1 = 0.1142$, $wR_2 = 0.2342$
Largest difference peak and hole (e Å^{-3})	0.76 and −0.66

[a] $R_1 = \Sigma||F_o|-|F_c||/\Sigma|F_o|$. $wR_2 = \{\Sigma[(F_o^2-F_c^2)^2]/\Sigma[w(F_o^2)^2]\}^{1/2}$; $w = 1/[\sigma^2(F_o^2)+(0.1197P)^2+1.8628P]$, where $P = (F_o^2+2F_c^2)/3$.

fraction of the second water molecule, O(1WA), form a pair of O–H···O bonds with one of the disordered perchlorate oxygen atoms, O(3B). Fig. 4 shows the schematic diagram of the hydrogen bonding pattern, $[Fe(MP_z3Pi)_2]ClO_4\cdot 2H_2O$ with the hydrogen bonds shown as dashed lines.

4. Supplementary material

Crystallographic data for the structure reported have been deposited with the Cambridge Crystallographic Data Centre, CCDC No. being 178366. Copies of this information may be obtained free of charge from The Director, CCDC Data Centre, 12 Union Road, Cambridge, CB2 1EZ, UK (fax: +44-1223-336033; e-mail: deposit@ccdc.cam.ac.uk or www: http://www.ccdc.cam.ac.uk).

Table 5
Selected bond distances (Å) and angles (°)

Bond lengths			
Fe–S1A	2.2235(16)	Fe–S1B	2.2169(14)
Fe–N1A	1.971(4)	Fe–N1B	1.966(4)
Fe–N2A	1.924(4)	Fe–N2B	1.922(4)
S1A–C6A	1.757(5)	S1B–C6B	1.754(5)
C5A–N2A	1.298(7)	C5B–N2B	1.293(7)
N2A–N3A	1.368(7)	N2B–N3B	1.380(6)
N3A–C6A	1.317(7)	N3B–C6B	1.320(6)
C6A–N5A	1.344(7)	C6B–N5B	1.343(6)
N1A–C4A	1.337(6)	N1B–C4B	1.336(7)
C4A–C5A	1.414(8)	C4B–C5B	1.443(8)
Bond angles			
S1A–Fe–N1A	163.79(12)	S1B–Fe–N1B	164.52(13)
S1A–Fe–N2A	84.30(15)	S1B–Fe–N2B	84.53(13)
S1A–Fe–N1B	89.61(14)	S1B–Fe–N1A	91.18(13)
S1A–Fe–N2B	95.42(13)	S1B–Fe–N2A	97.31(13)
N1A–Fe–N2A	79.95(18)	N1B–Fe–N2B	80.24(17)
N1A–Fe–N2B	100.20(17)	N1B–Fe–N2A	97.93(17)
N1A–Fe–N1B	88.80(18)	N2A–Fe–N2B	178.15(18)
S1A–Fe–S1B	94.60(6)		
Fe–S1A–C6A	96.32(19)	Fe–S1B–C6B	96.22(16)
Fe–N2A–N3A	123.9(3)	Fe–N2B–N3B	124.1(3)
Fe–N2A–C5A	117.0(4)	Fe–N2B–C5B	117.3(3)
C5A–N2A–N3A	119.0(4)	C5B–N2B–N3B	118.6(4)
N2A–N3A–C6A	112.9(4)	N2B–N3B–C6B	111.9(4)
N3A–C6A–N5A	118.3(5)	N3B–C6B–N5B	118.4(5)
N3A–C6A–S1A	122.1(4)	N3B–C6B–S1B	122.8(4)
N5A–C6A–S1A	118.8(4)	N5B–C6B–S1B	119.6(4)

Table 6
Hydrogen bonding distances (Å) and angles (°)

D–H···A	D–H	D···A	H···A	∠ D–H···A
N(4A)–H(4A)···O(2W)	0.73(4)	2.77(1)	2.05(4)	173(1)
N(4B)–H(4B)···O(1WA) [a]	0.79(5)	2.72(2)	1.95(5)	168(2)
O(2W)–H(2W1)···O(1B)^{i} [a]	0.74(4)	2.98(1)	2.27(5)	161(1)
O(2W)–H(2W2)···N(3B)^{i}	0.74(6)	2.97(1)	2.24(7)	167(4)
O(1WA) [a]–H(1WA)···O(3B)^{ii} [b]	0.75(6)	2.85(2)	2.38(5)	123(4)
O(1WA) [a]–H(2WA)···O(3B)^{ii} [b]	0.75(5)	2.85(2)	2.61(7)	102(4)

Symmetry equivalents: (i) $2-x$, $1-y$, $1-z$ (ii) x, $-1+y$, z.
[a] This refers to the major fraction in the disordered water molecule.
[b] This refers to the major fraction in the disordered perchlorate ion.

Acknowledgements

One of the authors (N.C.S.) is thankful to the University of Calcutta for providing the state-funded research fellowship during the tenure of this work. The authors are also thankful to Professor (Mrs.) A. Chatterjee, Programme Coordinator, Centre of Advanced Studies on Natural Products, Department of Chemistry, University of Calcutta, for providing the NMR spectrum and to Professor A. Patra, Department of Chemistry, University of Calcutta, for useful discussion on NMR spectral data.

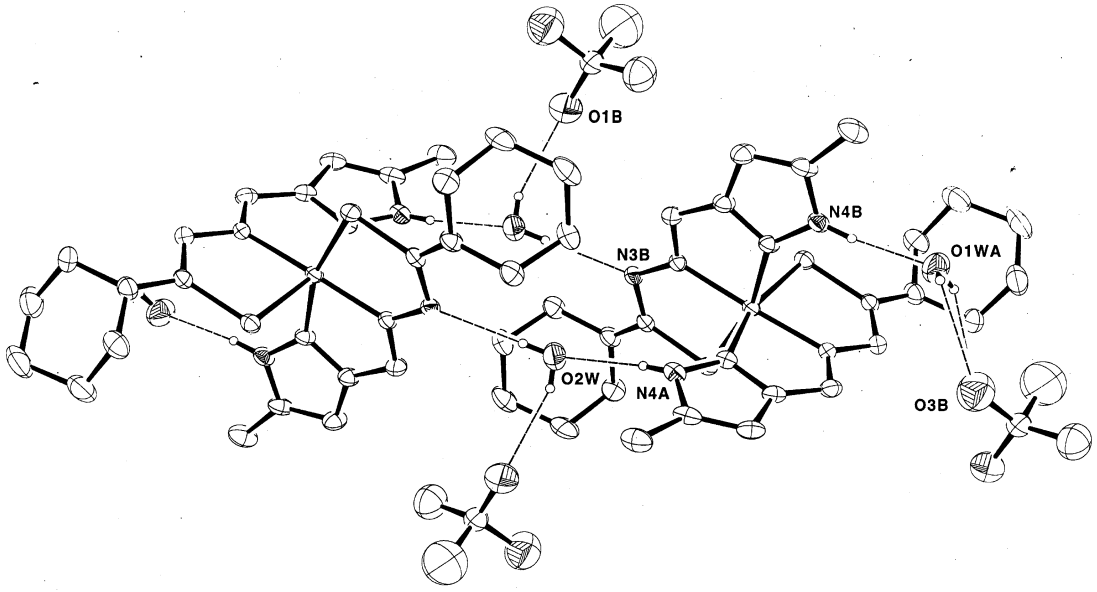

Fig. 4. Hydrogen bonding pattern in the crystal structure of $[Fe(MP_2 3Pi)_2]\ ClO_4 \cdot 2H_2O$. Donor and acceptor atoms involved in hydrogen bonding are shown by thermal ellipsoids with shaded octants. A few of the representative atoms have been labelled.

References

[1] D.L. Klayman, J.F. Bartosevich, T.S. Griffin, C.J. Mason, J.P. Scovill, J. Med. Chem. 22 (1979) 855.
[2] D.X. West, S.B. Padhye, P.B. Sonawane, Struct. Bonding 76 (1991) 1.
[3] A.E. Liberta, D.X. West, Biometals 5 (1992) 121.
[4] F.A. French, E.J. Blanz, Jr., J. Med. Chem. 13 (1970) 1117.
[5] (a) R. Raina, T.S. Srivastava, Inorg. Chim. Acta 67 (1982) 83;
(b) R. Raina, T.S. Srivastava, Ind. J. Chem. 22A (1983) 701.
[6] H. Beraldo, L. Tosi, Inorg. Chim. Acta 75 (1983) 249.
[7] (a) P. Bera, N. Saha, S. Kumar, D. Banerjee, R. Bhattacharya, Transition Met. Chem. 24 (1999) 425;
(b) N.C. Saha, A. Saha, R.J. Butcher, S. Chaudhuri, N. Saha, Inorg. Chim. Acta 339C (2002) 348, in press.
[8] (a) A. Mitra, T. Banerjee, P. Roychowdhury, S. Chaudhuri, P. Bera, N. Saha, Polyhedron 16 (1997) 3735;
(b) P. Bera, R.J. Butcher N. Saha, Chem. Lett. (1998) 559;
(c) N.C. Saha, A. Seal, R.J. Butcher, N. Saha, J. Ind. Chem. Soc. 78 (2002) 601;
(d) P. Bera, R.J. Butcher, S. Chaudhuri, N. Saha, Polyhedron 21 (2002) 1;
(e) N.C. Saha, R.J. Butcher, S. Chaudhuri, N. Saha, Polyhedron 21 (2002) 779.
[9] N. Saha, N. Mukherjee, Polyhedron 3 (1984) 1135.
[10] J.P. Scovill, Phosphorus, Sulfur Silicon 60 (1991) 15.
[11] G.M. Sheldrick, SHELX97, Program for the Refinement of Crystal Structure, University of Göttingen, Germany, 1997.
[12] D.T. Cromer, J.T. Weber, International Tables for X-ray crystallography, Table 2.2A, vol. IV, The Kynoch Press, Birmingham, UK, 1994.
[13] J.A. Ibers, W.C. Hamilton, Acta Crystallogr. 17 (1964) 781.
[14] M.A. Ali, M. Tarafder, J. Inorg. Nucl. Chem. 39 (1977) 1785.
[15] M.M. Mostafa, A. Hamid, A.M. Shallaby, A.A. El-Asmay, Transition Met. Chem. 6 (1981) 303.
[16] D.X. West, C.S. Carlson, K.J. Bouck, A.E. Liberta, Transition Met. Chem. (1991) 271.
[17] W.J. Geary, Coord. Chem. Rev. 7 (1971) 81.
[18] R.C. Agarwal, T.R. Rao, J. Inorg. Nucl. Chem. 40 (1978) 1177.
[19] J.R. Ferraro, Appl. Spectrosc. 23 (1969) 60.
[20] A.H. Ewald, R.L. Martin, E. Sinn, A.H. White, Inorg. Chem. 8 (1969) 1837.
[21] F.A. Cotton, Coord. Chem. Rev. 8 (1972) 185.
[22] R. Raina, T.S. Srivastava, Inorg. Chim. Acta 91 (1984) 137.
[23] D.X. West, P.M. Ahrweiler, G. Ertem, J.P. Scovill, D.L. Klayman, J.L. Flippen-Andeson, R. Gilardi, C. George, L.K. Pannell, Transition Met. Chem. 10 (1985) 264.
[24] B.S. Garg, M.R.P. Kurup, S.K. Jain, Y.K. Bhoon, Transition Met. Chem. 13 (1988) 247.
[25] (a) S.K. Jain, B.S. Garg, Y.K. Bhoon, Transition Met. Chem. 11 (1986) 89;
(b) S.K. Jain, B.S. Garg, Y.K. Bhoon, Spectrochim. Acta 42A (1986) 959.
[26] K. Nishida, S. Oshio, S. Kida, Inorg. Chim. Acta 23 (1977) 59.
[27] L.J. Farrugia, J. Appl. Crystallogr. 30 (1997) 565.
[28] K.A. Ketcham, J.K. Swearingen, A. Castiñeiras, I. Garcia, E. Bermejo, D.X. West, Polyhedron 20 (2001) 3265.
[29] D. Cremer, J.A. Pople, J. Am. Chem. Soc. 97 (1975) 1334.